Chem. Mater. **1996,** *8,* 777−782 777

Intercalation of Pyridine in Layered Titanates

Takayoshi Sasaki,* Fujio Izumi, and Mamoru Watanabe

National Institute for Research in Inorganic Materials, 1-1 Namiki, Tsukuba, Ibaraki 305, Japan

Received October 3, 1995. Revised Manuscript Received December 18, 1995[⊗]

The intercalation of pyridine has been examined for four types of layered protonic titanates such as $H_2Ti_3O_7$, $H_2Ti_4O_9\cdot 1.2H_2O$, $H_2Ti_5O_{11}\cdot 3H_2O$, and $H_xTi_{2-x/4}\square x/4O_4\cdot H_2O$ ($x \sim 0.7$, $\square$: vacancy). Upon the action of gaseous, liquid or aqueous pyridine at ambient temperature, the latter oxide peculiarly yielded a pyridine complex of composition $(C_5H_5N)_{0.3}H_x$-$Ti_{2-x/4}\square_{x/4}O_4\cdot 0.6H_2O$ while the other three materials did not. The intercalation compound lost weight in two steps of 40−120 and 120−320 °C, which were attributable to evaporation of interlayer water and of pyridine, respectively. Vibrational spectra suggested that pyridine was taken up as its protonated cationic form. Rietveld refinements demonstrated that the intercalation gave rise to an incommensurate gliding of neighboring host layers along the *a* axis (∼28% of its repeat unit) as well as an interlayer expansion. The pyridine ring is accommodated in an inclined way (∼64° with respect to the layer) having its nitrogen lone pair orientated parallel to the layer. The unique geometry of the interlayer gallery has the aromatic ring nestled into the corrugated host layers.

Introduction

Five types of layered alkali-metal titanates, $K_2Ti_2O_5$, $Na_2Ti_3O_7$, $K_2Ti_4O_9$, $Cs_2Ti_5O_{11}$, and $Cs_xTi_{2-x/4}\square_{x/4}O_4$ ($x \sim 0.7$, $\square$: vacancy), have been synthesized.[1−5] The latter four compounds can be converted into their acid-exchanged forms preserving their host framework (see Figure 1).[6−10] The resulting protonic oxides, $H_2Ti_3O_7$, $H_2Ti_4O_9\cdot 1.2H_2O$, $H_2Ti_5O_{11}\cdot 3H_2O$, and $H_xTi_{2-x/4}\square_{x/4}O_4\cdot H_2O$, undergo ion-exchange and intercalation reactions at ambient temperature. A number of papers have documented on their ion-exchange behavior,[11−13] pillaring,[14,15] and preparation of organic/inorganic complexes.[16,17] However, there have been few studies that systematically report the intercalation of pyridine. The reactivity with pyridine is of great importance since pyridine, the weak base, is a nice probe for the relative strength of the solid acidity.

Examination on crystal structures of pyridine intercalation compounds is another attractive motive point. Although the intercalation of pyridine has been extensively investigated for a wide variety of layered hosts,[18−21] structural aspects, particularly on an accommodation manner of the guest in interlayer galleries, have not been fully appreciated. Some distinctive configuration models, parallel and perpendicular orientation of the aromatic ring (see Figure 2), have been proposed mostly on the basis of a difference in interlayer spacing before and after the intercalation and, further in some cases, one-dimensional Fourier maps from neutron diffraction profiles[22] and NMR study.[23] However, there still remains some structural ambiguity; for example, whether there is some tilting of the ring away from parallel or perpendicular orientation or whether pyridine is nestled into host layers, and, if so, how. These information will get insight into host−guest interactions. Therefore, the

---

[⊗] Abstract published in *Advance ACS Abstracts,* February 1, 1996.

(1) Andersson, S.; Wadsley, A. D. *Acta Chem. Scand.* **1961**, *15*, 663.

(2) Andersson, S.; Wadsley, A. D. *Acta Crystallogr.* **1961**, *14*, 1245.

(3) (a) Verbaere, A.; Tournoux, M. *Bull. Soc. Chim. Fr.* **1973**, *4*, 1237. (b) Dion, M.; Piffard, Y.; Tournoux, M. *J. Inorg. Nucl. Chem.* **1978**, *40*, 917.

(4) (a) Grey, I. E.; Madsen, I. C.; Watts, J. A.; Bursill, L. A.; Kwiatkowska, J. *J. Solid State Chem.* **1985**, *58*, 350. (b) Kwiatkowska, J.; Grey, I. E.; Madsen, I. C.; Bursill, L. A. *Acta Crystallogr.* **1987**, *B43*, 258.

(5) (a) Hervieu, M.; Raveau, B. *Rev. Chim. Miner.* **1981**, *18*, 642. (b) Grey, I. E.; Madsen, I. C.; Watts, J. A. *J. Solid State Chem.* **1987**, *66*, 7.

(6) (a) Sasaki, T.; Komatsu, Y.; Fujiki, Y. *Solvent Extr. Ion Exch.* **1983**, *1*, 775. (b) Bamberger, C. E.; Begun, G. M.; MacDougall, C. S. *Appl. Spectrosc.* **1990**, *44*, 30.

(7) (a) Izawa, H.; Kikkawa, S.; Koizumi, M. *J. Phys. Chem.* **1982**, *86*, 5023. (b) Feist, T. P.; Mocarski, S. J.; Davies, P. K.; Jacobson, A. J.; Lewandowski, J. T. *Solid State Ionics* **1988**, *28−30*, 1338. (c) Feist, T. P.; Davies, P. K. *J. Solid State Chem.* **1992**, *101*, 275.

(8) (a) Marchand, R.; Brohan, L.; Tournoux, M. *Mater. Res. Bull.* **1980**, *15*, 1129. (b) Sasaki, T.; Watanabe, M.; Komatsu, Y.; Fujiki, Y. *Inorg. Chem.* **1985**, *24*, 2265.

(9) Sasaki, T.; Komatsu, Y.; Fujiki, Y. *Chem. Mater.* **1992**, *4*, 894.

(10) (a) Sasaki, T.; Komatsu, Y.; Fujiki, Y. *J. Chem. Soc., Chem. Commun.* **1991**, 817. (b) Sasaki, T.; Watanabe, M.; Michiue, Y.; Komatsu, Y.; Izumi, F.; Takenouchi, S. *Chem. Mater.* **1995**, *7*, 1001.

(11) (a) Izawa, H.; Kikkawa, S.; Koizumi, M. *J. Solid State Chem.* **1985**, *60*, 264. (b) Izawa, H.; Kikkawa, S.; Koizumi, M. *J. Solid State Chem.* **1987**, *69*, 336.

(12) (a) Sasaki, T.; Watanabe, M.; Komatsu, Y.; Fujiki, Y. *Bull. Chem. Soc. Jpn.* **1985**, *58*, 3500. (b) Sasaki, T.; Komatsu, Y.; Fujiki, Y. *Mater. Res. Bull.* **1987**, *22*, 1321. (c) Sasaki, T.; Komatsu, Y.; Fujiki, Y. *Inorg. Chem.* **1989**, *28*, 2776.

(13) England, W. A.; Birkett, J. E.; Goodenough, J. B.; Wiseman, P. J. *J. Solid State Chem.* **1983**, *49*, 300.

(14) (a) Anderson, M. W.; Klinowski, J. *Inorg. Chem.* **1990**, *29*, 3260. (b) Landis, M. E.; Aufdembrink, B. A.; Chu, P.; Johnson, I. D.; Kirker, G. W.; Rubin, M. K. *J. Am. Chem. Soc.* **1991**, *113*, 3189.

(15) (a) Cheng, S.; Wang, T. *Inorg. Chem.* **1989**, *28*, 1283. (b) Sylvester, P.; Cahill, R.; Clearfield, A. *Chem. Mater.* **1994**, *6*, 1890. (c) Hou, W.; Yan, Q.; Peng, B.; Fu, X. *J. Mater. Chem.* **1995**, *5*, 109.

(16) Izawa, H.; Kikkawa, S.; Koizumi, M. *Polyhedron* **1983**, *2*, 741.

(17) (a) Clément, P.; Marchand, R. *C. R. Acad. Sci. Paris Ser. II* **1983**, *296*, 1161. (b) Miyata, H.; Sugahara, Y.; Kuroda, K.; Kato, C. *J. Chem. Soc., Faraday Trans. 1* **1988**, *84*, 2677.

(18) *Intercalation Chemistry*; Whittingham, M. S., Jacobson, A. J., Eds.; Academic Press: New York, 1982.

(19) (a) Odink, D. A.; Song, K.; Kauzlarich, S. M. *Chem. Mater.* **1992**, *4*, 906. (b) Song, K.; Kauzlarich, S. M. *Chem. Mater.* **1994**, *6*, 386.

(20) Kinomura, N.; Kumada, N. *Solid State Ionics* **1992**, *51*, 1.

(21) Joy, P. A.; Vasudenvan, S. *J. Am. Chem. Soc.* **1992**, *114*, 7792.

(22) Riekel, C.; Fischer, C. O. *J. Solid State Chem.* **1979**, *29*, 181.

(23) McDaniel, P. L.; Barbara, T. M.; Jonas, J. *J. Phys. Chem.* **1988**, *92*, 626.

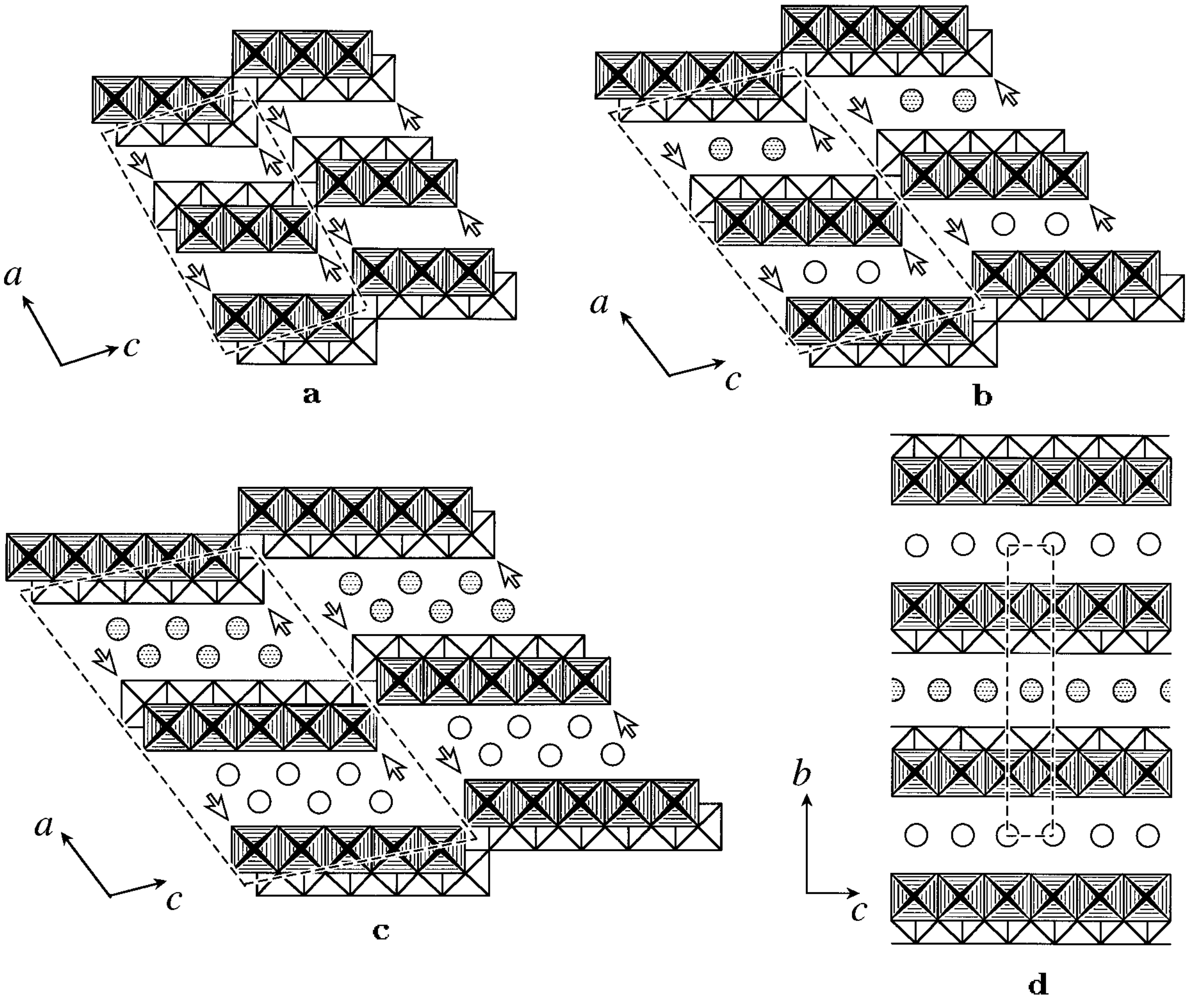

Figure 1. Schematic representation of crystal structures for the layered protonic oxides: (a, top left) $H_2Ti_3O_7$ (trititanate), (b, top right) $H_2Ti_4O_9{\cdot}1.2H_2O$ (tetratitanate), (c, bottom left) $H_2Ti_5O_{11}{\cdot}3H_2O$ (pentatitanate), (d, bottom right) $H_xTi_{2-x/4}\square_{x/4}O_4{\cdot}H_2O$ (lepidocrocite-related titanate). The unit cells (enclosed by broken lines) are *C*-base-centered monoclinic for $H_2Ti_3O_7$, $H_2Ti_4O_9{\cdot}1.2H_2O$ and $H_2Ti_5O_{11}{\cdot}3H_2O$, and body-centered orthorhombic for $H_xTi_{2-x/4}\square_{x/4}O_4{\cdot}H_2O$. Circles and arrows denote H_2O (or H_3O^+) and position of hydroxylated proton, respectively. In $H_2Ti_3O_7$, another equivalent of protons besides indicated ones (terminal hydroxyls) is situated in the interlayer space.

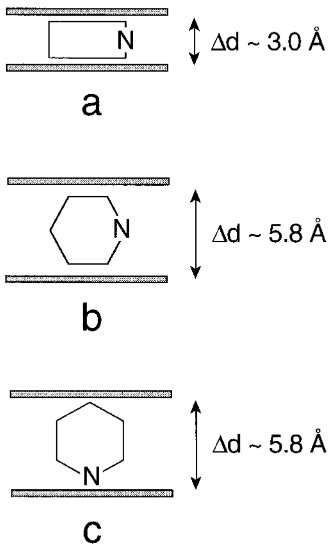

Figure 2. Accommodation modes of pyridine in layered hosts: (a) parallel, (b), (c) perpendicular orientation.

present study is undertaken to clarify structural details of a pyridine complex by a full structure analysis as well as to obtain information on the Brønsted acidity for this series of the protonic titanates.

Experimental Section

Reagents and Materials. Layered alkali-metal titanates were prepared by conventional solid-state reactions.[2,5–10] A stoichiometric mixture of alkali-metal carbonates (Rare Metallic Co., >99.9% purity) and TiO_2 (99.98%) was calcined at 900 °C for $Na_2Ti_3O_7$, 1000 °C for $K_2Ti_4O_9$, and $Cs_2Ti_5O_{11}$, 800 °C for $Cs_xTi_{2-x/4}\square_{x/4}O_4$. The obtained polycrystalline materials were converted into their protonated forms by being immersed in a 1 mol dm^{-3} HCl solution (solid-to-solution ratio: 20 g dm^{-3}). The repeated treatments (24 h × 5) achieved a nearly complete removal of interlayer alkali-metal ions. The solid was washed with distilled water by decantation until a pH value of the supernatant solution exceeded 5. The resulting protonated titanates were retrieved by filtration and dried over a saturated NaCl solution (70% relative humidity). X-ray diffraction (XRD) data and water contents were consistent with those from literatures.[7–10]

Intercalation Procedures. The intercalation of pyridine was attempted by treating the protonic titanates with (i) vapor, (ii) neat liquid, and (iii) aqueous solution. For i, the materials and liquid pyridine were separately put in a vessel, and then air was replaced with N_2 gas. The system was maintained at 35 ± 1 °C for 5 days, allowing vaporized pyridine to interact with solids. For ii and iii, a weighed amount (0.2 g) of the titanates was shaken with 20 cm^3 of a neat or aqueous (1/1) solution of pyridine at 25 ± 1 °C for 7 days. The solid phase was collected by filtration, washed with acetone, and dried in air.

The intercalation of substituted pyridines, 2-methyl, 3-methyl, 4-methyl, 4-ethyl, and 4-propyl compounds, was examined similarly by the procedure ii.

Characterizations. Powder XRD data were collected on a Rigaku RAD-2B diffractometer with graphite-monochromatized Cu Kα radiation ($\lambda = 1.5405$ Å). Unit-cell dimensions were determined by a least-squares procedure.[24] Rietveld refinements were carried out on step-scanned intensity data using the latest version of RIETAN,[25] which employs the asymmetric pseudo-Voigt function for profile shape fitting. This is competent to handle with diffraction data for layered materials which sometimes exhibit severe anisotropic broadening for a particular direction. FT-IR spectra for a sample in KBr pellet were recorded in the range 400−4000 cm^{-1} with a resolution of 2 cm^{-1} (Digilab S-45 spectrophotometer). Thermogravimetric measurements were performed at a heating rate of 10 °C min^{-1} under a N_2 gas purge (Mac science 2000S thermal analyzer), and evolved gas was simultaneously identified by monitoring FT-IR spectra. Elemental analyses were carried out as follows:[26] A weighed amount of the intercalation compounds was dissolved with a H_2SO_4 solution. Its Ti content was determined by gravimetry as TiO_2 from cupferron precipitation and Cs was by atomic absorption spectroscopy. The contents for C, H, and N were obtained by combustion of the materials followed by gas chromatography determination (Perkin Elmer 2400-type CHNS/O analyzer).

Results and Discussion

Preparation of the Pyridine Intercalation Compounds. Among the four kinds of protonic titanates, $H_xTi_{2-x/4}\square_{x/4}O_4\cdot H_2O$ peculiarly took up pyridine. All the three modes of interaction produced the identical results. The elemental analyses and XRD data provided definitive evidence for the intercalation. The composition was determined to be $(C_5H_5N)_{0.3}H_{0.7}Ti_{1.825}\square_{0.175}O_4\cdot 0.6H_2O$. Calcd: Ti, 46.8%; C, 9.7%; H, 1.8%; N, 2.3%. Found: Ti, 45.8%; C, 10.3%; H, 1.8%; N, 2.4%.[26] Neither prolonged treatments nor interaction at elevated temperatures drove the reaction beyond this loading level. The incomplete neutralization of interlayer protons by pyridine is associated with steric restrictions, which will be described later.

Upon the pyridine uptake, the interlayer distance expanded from 9.4 to 11.4 Å as depicted in Figure 3. The increment of 2.0 Å appeared to be small in comparison with values expected for the molecular size of pyridine. One should pay attention to the fact that $H_xTi_{2-x/4}\square_{x/4}O_4\cdot H_2O$ accommodates interlayer H_2O molecules, 70% of which are in the form of H_3O^+ ions. The compositional change suggests that pyridine was incorporated by one-to-one substitution of H_2O molecule. This may not bring about a considerable expansion of the gallery height. The titanate, $H_xTi_{2-x/4}\square_{x/4}O_4\cdot H_2O$, lost the interlayer water by being heated up to 140 °C to produce a dehydrated phase, $H_xTi_{2-x/4}\square_{x/4}O_4$ ($x = 0.70$), the interlayer spacing of which was 6.6 Å.[10] Since the size of proton is negligibly small, the difference of 4.8 Å (=11.4 − 6.6) can be taken for a net expansion. This magnitude is comparable to or slightly smaller than the diameter of pyridine molecule (∼5.8 Å), which suggests a nearly perpendicular orientation with respect to the host layer (similar to Figure 2b or c). A detailed accommodation manner will be described below.

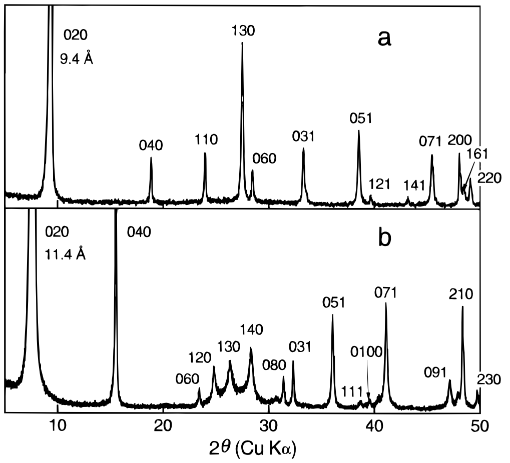

Figure 3. XRD patterns of $H_xTi_{2-x/4}\square_{x/4}O_4\cdot H_2O$ (a) before and (b) after the treatment with pyridine.

Table 1. Chemical Compositions and Lattice Constants for the Pyridine Complexes

guest	stoichiometry[a]	a/Å	b/Å	c/Å
pyridine	0.30	3.7864(8)	22.722(5)	2.9797(6)
4-methylpyridine	0.28	3.7898(7)	22.730(6)	2.9764(5)
4-ethylpyridine	0.25	3.7858(11)	23.087(6)	2.9833(6)
4-propylpyridine	0.23	3.7808(10)	23.034(7)	2.9826(8)
b		3.783(2)	18.735(8)	2.978(2)

[a] Contents of pyridine or substituted pyridines per formula weight of the host. [b] $H_xTi_{2-x/4}\square_{x/4}O_4\cdot H_2O$ for a comparison use.

The intercalation of substituted pyridines in $H_xTi_{2-x/4}\square_{x/4}O_4\cdot H_2O$ was also examined. Pyridine derivatives with substituents at the 4-position were taken up while 2- or 3-methyl compounds were not or in only a limited way. Table 1 lists the stoichiometry and cell parameters for the obtained complexes.

On the other hand, the intercalation of pyridine into $H_2Ti_3O_7$, $H_2Ti_4O_9\cdot 1.2H_2O$, and $H_2Ti_5O_{11}\cdot 3H_2O$ was unsuccessful. No change was observed when treated with an aqueous pyridine solution. On the action of vaporized or liquid pyridine, the interlayer spacing shrank from 9.1 to 8.0 Å for $H_2Ti_4O_9\cdot 1.2H_2O$ and from 10.4 to 8.3 Å for $H_2Ti_5O_{11}\cdot 3H_2O$. These changes were not attributable to incorporation of pyridine but to dehydration. The XRD patterns were very similar to those for $H_2Ti_4O_9$ and $H_2Ti_5O_{11}\cdot H_2O$ which were obtained by heating $H_2Ti_4O_9\cdot 1.2H_2O$ and $H_2Ti_5O_{11}\cdot 3H_2O$ at 100 °C, respectively.[8,9] The TGA-IR analyses also supported no intercalation, detecting only trace quantities of pyridine. The results above conclude that $H_xTi_{2-x/4}\square_{x/4}O_4\cdot H_2O$ possesses the strongest solid acidity in comparison with the other titanates.

There are a number of protonic niobates and titanoniobates, the layer architectures of which are, more or less, analogous to those of the titanates studied here. Reactivities of these materials towards organic bases with various pK_a have been explored, from which it is suggested that the Brønsted acidity generally increases in the order of titanates < titanoniobates < niobates.[27−31] This tendency has been explained by the nature of

---

(24) Appleman, D. E.; Evans, H. T., Jr. Report No. PB216188, U. S. Dept. of Commerce, National Technical Information Service: Springfield, VA, 1973.

(25) (a) Izumi, F. *The Rietveld Method*; Young, R. A., Ed.; Oxford University Press: Oxford, 1993. (b) Kim, Y.-I.; Izumi, F. *J. Ceram. Soc. Jpn.* **1994**, *102*, 401.

(26) Sumika Analytical Laboratory, Niihama, Ehime 792, Japan.

(27) Rebbah, H.; Borel, M. M.; Bernard, M.; Raveau, B. *Rev. Chim. Miner.* **1981**, *18*, 109.

(28) Jacobson, A. J.; Johnson, J. W.; Lewandowski, J. T. *Mater. Res. Bull.* **1987**, *22*, 45.

(29) Gopalakrishnan, J.; Bhat, V. *Mater. Res. Bull.* **1987**, *22*, 413.

(30) Bhat, V.; Gopalakrishnan, J. *Solid State Ionics* **1988**, *26*, 25.

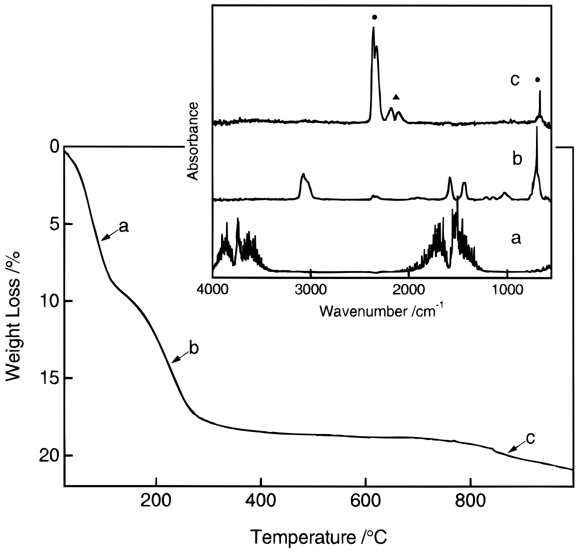

Figure 4. Thermogravimetric curve for the pyridine intercalation compound. The FT-IR spectra in the inset are for volatile components at (a) 94, (b) 224, and (c) 865 °C, which were identified as H_2O, pyridine, and CO_2 (●) + CO (▲), respectively.

functional groups, M−O−H; a higher valent central metal, M, brings about a stronger acidity. It is noteworthy that none of the titanates has been reported to intercalate pyridine[17a] before the present study demonstrates that $H_xTi_{2-x/4}\square_{x/4}O_4\cdot H_2O$ does. The intercalation ability, or the overall acidity of solid acids, should be governed by their structural features as well as the acidity of a functional group itself. One of the most dominating structural factors may be a negative charge density of layers. Penetration of guests into higher layer charged compounds will be more difficult than that into lower charged ones. The layer charge density for $H_xTi_{2-x/4}\square_{x/4}O_4\cdot H_2O$ (1/32.2 Å^{-2}) is the lowest in the series of the titanates (1/17.2 Å^{-2} for $H_2Ti_3O_7$, 1/22.5 Å^{-2} for $H_2Ti_4O_9\cdot 1.2H_2O$, 1/28.2 Å^{-2} for $H_2Ti_5O_{11}\cdot 3H_2O$),[10] which probably makes the intercalation into $H_xTi_{2-x/4}\square_{x/4}O_4\cdot H_2O$ most feasible.

Characterization of the Pyridine Intercalation Compound. Figure 4 shows the typical weight loss profile of the pyridine complex. Noticeable two-stepped losses (step I, 40−120 °C, step II, 120−320 °C) were observed although they were not perfectly resolved. The in situ FT-IR analyses identified water and pyridine as predominant species released in step I and II, respectively. The layer structure was preserved at the end of step I without a considerable change in interlayer separation. The removal of pyridine in step II collapsed the layer structure and the titanium dioxide (anatase) started to crystallize above 300 °C. The weight loss in step II was lower than an expected value based on the chemical composition, indicative of incomplete elimination of pyridine. Actually, the thermogravimetric curve showed a gradual weight loss in a higher temperature region, which was accelerated above 800 °C. A considerable amount of CO_2 and CO was detected during the process as shown in the inset of Figure 4. This phenomenon as well as the gray color of the sample (200−800 °C) strongly suggests that some portion of pyridine was turned into a carbonaceous substance which was liberated as carbon oxides taking oxygen from the titanium dioxide.

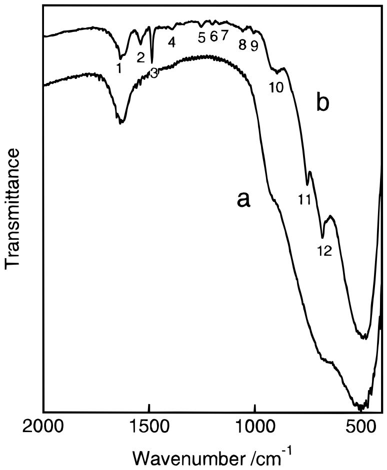

Figure 5. FT-IR spectra of $H_xTi_{2-x/4}\square_{x/4}O_4\cdot H_2O$ (a) before and (b) after the treatment with pyridine: (1) 1635 cm^{-1}, (2) 1541, (3) 1486, (4) 1390, (5) 1254, (6) 1198, (7) 1167, (8) 1057 (9) 1007, (10) 896, (11) 755, 12: 682.

The vibrational spectra provided the information on the nature of incorporated pyridine. A number of infrared absorptions appeared upon intercalation (see Figure 5). The bands occurring at 682, 1007, 1198, and 1635 cm^{-1} are diagnostic to pyridinium ion.[32] On the other hand, the presence of neutral pyridine was inconclusive because its characteristic absorption bands (694−699, 1446−1448, and 1574−1576 cm^{-1})[32] were not discernible. Therefore, the chemical composition may be formulated as $0.3C_5H_5NH^+\cdot 0.4H_3O^+\cdot 0.2H_2O\cdot Ti_{1.825}\square_{0.175}O_4^{0.7-}$, where first three terms represent interlayer guest species. This mode of bonding is consistent with the Brønsted acidic nature of the host material.

Crystal Structure of the Pyridine Complex. The incorporation of pyridine brought about a change in space group from *Immm* to *Pnn*2 or *Pnnm*. Reflections of 0*kl* with $k + l \neq 2n$ and *h*0*l* with $h + l \neq 2n$ were systematically absent for the pyridine complex while those of *hkl* with $h + k + l \neq 2n$ were extinct for $H_xTi_{2-x/4}\square_{x/4}O_4\cdot H_2O$ before the intercalation (see Figure 3). The symmetry change can be accounted for by a lateral displacement of adjacent host layers with respect to one another along the *a* axis, the magnitude of which is not multiples of half of the *a* dimension.

The XRD data in Figure 3 was of relatively high quality to be analyzed by Rietveld profile fitting. Table 2 summarizes the experimental procedures and crystallographic data. The higher symmetry, *Pnnm*, was adopted. Initial positional parameters for Ti and O atoms were obtained from the ideal drawing of the lepidocrocite-type layers. A magnitude of the shift of the host layers was roughly estimated to be ~1 Å by means of intensity simulation starting from the body-centered lattice. The refinement based on the model comprising the host layers only converged satisfactorily (R_{wp} = 0.125), giving TiO_6 octahedron of reasonable dimensions. A Fourier synthesis at this stage located four of carbon atoms on the pyridine ring. On the other hand, the position of H_2O molecules could not be

---

(31) Gopalakrishnan, J.; Uma, S.; Bhat, V. *Chem. Mater.* **1993**, *5*, 132.

(32) Salmon, A.; Eckert, H.; Herber, H. *J. Chem. Phys.* **1984**, *81*, 5206.

Table 2. Refinement Procedures and Crystallographic Data for the Pyridine Complex

chemical formula	$(C_5H_5N)_{0.3}H_{0.7}Ti_{1.825}$-$\square_{0.175}O_4 \cdot 0.6H_2O$
angular range, 2θ/deg	30−100
step scan increment, 2θ/deg	0.03
count time/s	8
no. of scans	5
space group	*Pnnm* (No. 58)
Z	2
C−N distance and tolerance/Å	1.390(25)
C−C distance and tolerance/Å	1.390(25)
C−N−C angle and tolerance/deg	120(5)
$R_{wp} = [\Sigma w(y_o - y_c)^2/\Sigma(wy_o^2)]^{1/2}$	0.098
$R_p = (\Sigma\lvert y_o - y_c\rvert/\Sigma y_c)$	0.078
$R_I = \Sigma\lvert I_o - I_c\rvert/\Sigma I_o$	0.036
$R_F = \Sigma\lvert I_o^{1/2} - I_c^{1/2}\rvert/\Sigma I_o^{1/2}$	0.019
$R_{exp} = [(N_p - N_r - N_c)/\Sigma(wy_o^2)]^{1/2}$ [a]	0.032

[a] N_p: number of intensity data. N_r: number of refined parameters. N_c: number of constraints.

Table 3. Fractional Coordinates and Isotropic Temperature Factors for the Pyridine Complex

atom	position	occupancy	*x*	*y*	*z*	B/Å^2
C/N[a]	4*e*	0.3	0.5	0.5	0.043(66)	7.6(35)
C	8*h*	0.3	0.356(30)	0.451(4)	0.263(18)	7.6[b]
Ti	4*g*	0.9125	0.344(2)	0.2054(3)	0.0	1.4(3)
O1	4*g*	1.0	0.339(6)	0.1609(10)	0.5	1.0[c]
O2	4*g*	1.0	0.349(5)	0.2754(10)	0.5	1.0[c]

[a] Virtual species of (0.5C + 0.5N). [b] Constrained to be equal to *B* for C/N. [c] Fixed.

Table 4. Selected Interatomic Distances (Å) and Bond Angles (deg)

		TiO_6 Octahedron			
Ti−O1	(×2)	1.80(1)	O1−O2	(×2)	2.60(2)
Ti−O2	(×2)	2.18(2)	O1−O1[c]	(×2)	2.9784(9)
Ti−O2[a]	(×1)	1.96(2)	O1−O2[a]	(×2)	2.83(3)
Ti−O2[b]	(×1)	1.92(2)	O1−O2[b]	(×2)	2.79(3)
mean		1.97	O2−O2[a]	(×4)	2.67(2)
			mean		2.76
Pyriding Ring to Host Layer			Pyridine Ring		
C−O1[a]		3.23(9)	C−C		1.41(11)
C−O1[b]		3.30(10)	C−C/N		1.40(12)
C−O2		4.05(9)	C−C/N−C		124(15)
			C−C−C/N		118(7)

[a] $^1/_2 + x, {}^1/_2 - y, {}^1/_2 - z$. [b] $-^1/_2 + x, {}^1/_2 - y, {}^1/_2 - z$. [c] $x, y, 1 + z$.

determined. It is postulated that the heterocyclic ring is orientated in such a way that its C_2 axis coincides with the 2-fold axis of the lattice ($x = y = 0$ and 0.5), which is similar to the configuration in Figure 2b. Parallel and antiparallel alignments should be statistical due to the restriction from the space group (mirror plane at $z = 0$ and 0.5). This mode of accommodation instead of that analogous to Figure 2c is compatible with the lattice expansion for the substituted pyridine intercalation compounds.[33] The gallery height (=b/2, see Table 1) was nearly independent of the chain length of the substituted groups at the 4-position of the ring. The refinement including pyridine required to impose soft constraints on the hexagonal shape of the ring (see Table 2).

The final structure is visualized in Figure 6, and its atomic coordinates are tabulated in Table 3. Bond lengths and angles are listed in Table 4. The introduction of pyridine considerably modified a geometry of the gallery. A highly symmetrical coordination environment (a pseudocubic cavity) before the reaction was transformed to a distorted one (an elongated parallelepiped). The chemical formula described above, $0.3C_5H_5NH^+ \cdot 0.4H_3O^+ \cdot 0.2H_2O \cdot Ti_{1.825}\square_{0.175}O_4^{0.7-}$, means that 30% of the parallelepiped cavities are occupied by pyridinium ions and remaining by H_2O molecules or H_3O^+ ions. The partial loading of pyridine is ascribed

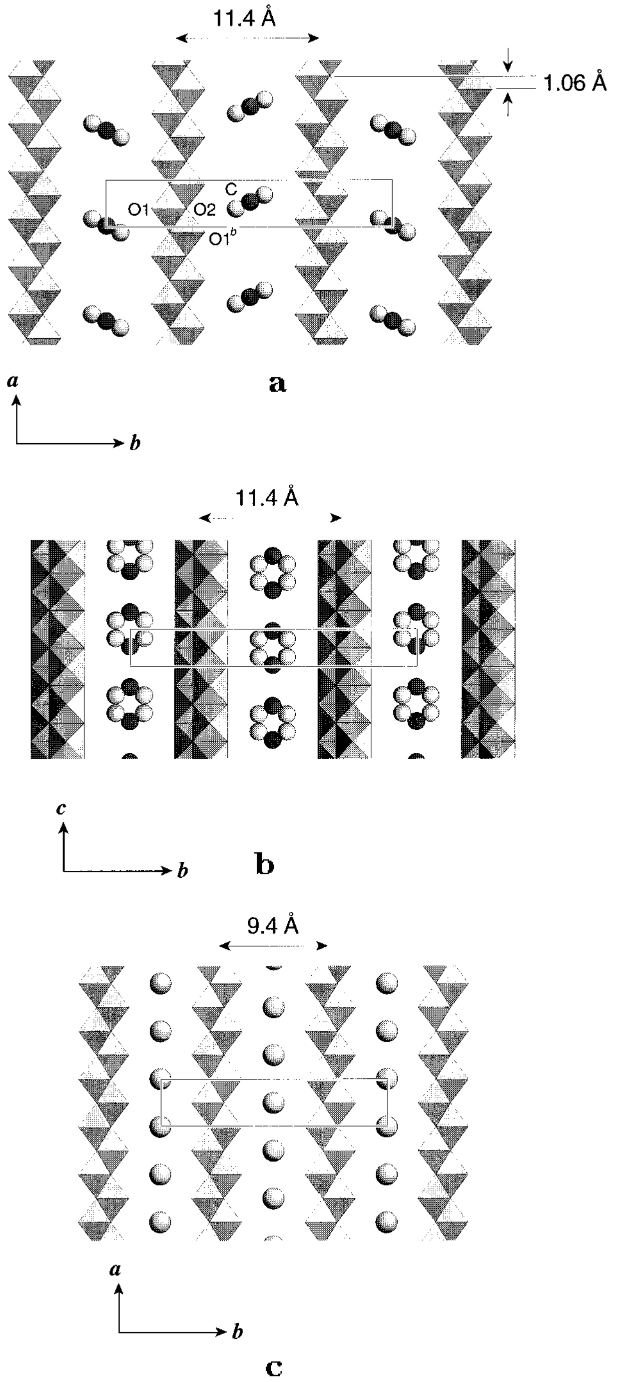

Figure 6. Crystal structure for the pyridine complex viewed down along the (a, top) *c* and (b, middle) *a* axis. The corresponding view of $H_xTi_{2-x/4}\square_{x/4}O_4 \cdot H_2O$ is depicted in (c, bottom) for a comparison use. The unit cell is encircled. Lighter and darker circles in (a) and (b) represent carbon atoms and virtual species of (0.5C + 0.5N), respectively. Distribution of pyridine is tentative; every second cavity both along the *a* and *c* axes is occupied, making total occupancy to be $^1/_4$. The open space may be situated by H_2O. Circles in (c) denotes H_2O and H_3O^+.

---

[33] The orientation of the nitrogen lone pair could not be determined by the refinements themselves. Incorporation of the pyridine ring in both alignment modes (similar to Figure 2b,c) gave similar reliability parameters.

to the steric effect; pyridine molecule cannot be accommodated within a single cavity but protrudes out of it. This makes occupation of two neighboring sites intolerable.

The aromatic ring is tilted by 26° from the layer normal. This orientation may be a consequence of interplay between electrostatic force of the system and efficient packing of pyridine. The orientation of pyridine in a variety of layered hosts has been a controversial topic.[18−23] In most of the cases, extreme configurations, namely, parallel and perpendicular orientation, have been discussed solely on the basis of a lattice expansion in comparison with the guest size. However, such a simple estimation may not always deduce an accurate accommodation fashion. This study has clearly demonstrated that the intermediate orientation is possible.

The pyridine ring is evidently nestled into periodical corrugations of the host layers. There may be some weak interaction between pyridine and O1 atom through hydrogen on the aromatic ring. It is reasonable to presume that the molecular shape of pyridine, especially with regards to C−H bonds, is virtually unchanged after the intercalation. If so, the C−H bonds point at O1 atoms in a nearly straight manner. The C−O1 interatomic distance of 3.3 Å also suggests the interaction, being slightly shorter than a sum of the bond length of C−H (1.08 Å), the van der Waals radius for hydrogen (1.2 Å) and the ionic one for oxygen (1.4 Å).[34,35]

CM950463H

---

(34) *Tables of Interatomic Distances and Configurations in Molecules and Ions*; Sutton, L. E., Ed.; The Chemical Society Special Publication, No. 11: London, 1958.

(35) *Handbook of Chemistry and Physics*, Weast, R. C., Ed.; CRC Press: Cleveland, 1974.